

THE EFFECT OF Ag CONTENT AND HEAT TREATMENT ON STRUCTURAL AND MORPHOLOGICAL PROPERTIES OF THIN $(\text{Cu}_{1-x}\text{Ag}_x)_2\text{ZnSnSe}_4$ FILMS

H. I. MOHAMMED^{a*}, I. H. KHDAYER^b, I. S. NAJI^c

^aCollege of Education for pure Science_Ibn Al-Haitham, University of Baghdad, Iraq

^bCollege of Education for pure Science_Ibn Al-Haitham, University of Baghdad, Iraq

^cCollege of Science, University of Baghdad, Iraq

$(\text{Cu}_{1-x}\text{Ag}_x)_2\text{ZnSnSe}_4$ alloys have been fabricated with different Ag content ($x=0, 0.1, \text{ and } 0.2$) successfully from their elements. Thin films of these alloys have been deposited on coring glass substrate at room temperature by thermal evaporation technique under vacuum of 10^{-5} Torr with thickness of 800nm and deposition rate of 0.53 nm/sec. Later, films have been annealed in vacuum at (373, and 473)K, for one hour. The crystal structure of fabricated alloys and as deposited thin films had been examined by XRD analysis, which confirms the formation of tetragonal phase in [112] direction, and no secondary phases are founded. The shifting of main polycrystalline peak (112) to lower Bragg's angle as compared to $\text{Cu}_2\text{ZnSnSe}_4$ angle refers to incorporation of Ag in the lattice. Annealing films adopt the similar structure, but peaks become sharper and more intensity, and crystallizing increase with increasing annealing temperature. AFM images confirms that all thin CAZTSe films are polycrystalline in nature and demonstrated that the size of grains increases with increasing Ag content and annealing temperature.

(Received October 21, 2019; Accepted March 6, 2020)

Keywords: $\text{Cu}_2\text{ZnSnSe}_4$ films, Structural properties, Morphological properties, Ag content, Heat treatment

1. Introduction

Currently free indium $\text{Cu}_2\text{ZnSnSe}_4$ compound, which returns to $\text{I}_2\text{-II-IV-VI}_4$ semiconductor group is founded to be candidate material for low cost solar cell absorber[1,2], due to it has many features involving suitable direct energy gap (1.5 eV) , high absorbance, high stability for radiation, cheap components, and very low toxicity[3-6].

Thin CZTSe films can be fabricated by vacuum and non-vacuum methods such as: co-evaporation[7], electro deposition[8], evaporation and vapor phase selenization[9], pulsed laser[10], spin coating[11], and RF magnetron sputtering [12]. Vacuum methods such as evaporation are suitable for industrialized productions, stable, able to fabricate CZTSe solar cell with high efficiency, and can simply tuned the stoichiometric ratio in CZTSe films during process [13].

$\text{I}_2\text{-II-IV-VI}_4$ quaternary chalcogenide semiconductor compounds such as CZTSe exhibit one of the three crystal structures: kesterite(KS), stannite(ST), and primitive mixed CA(PMCA) structure. KS structure is obtained from I-III-VI_2 ternary compound with chalcopyrite(CH) structure, while ST and PMCA structures are obtained from I-III-VI_2 ternary compound with CuAu-like(CA) structure[2,14]. So, CZTSe compound comes from CuInSe_2 by substituting 50% of Indium with zinc and substituting the remaining ratio of indium with tin [12].

Thin CZTSe films solar cell possess a good photoconversion efficiency but, it is remaining lower than photoconversion efficiency of commercial photovoltaic cells due to deficit in V_{oc} which resulting from formation of Cu_{Zn} antisite defects in high concentration because of their low formation energy due to the similar ionic radius of Cu and Zn[15,16].

* Corresponding authors: moonbb_moonaaaa@yahoo.com

To solve this problem Ag is a promising element for substituting Cu, because Cu and Ag are of the same group in the periodic table, and Ag has larger atomic radius, therefore a higher energy needed for defect formation [17].

This paper study the effect of Ag content on the structural and morphological properties of as deposited and annealed thin $(\text{Ag}_x\text{Cu}_{1-x})_2\text{ZnSnSe}_4$ films which grown on glass substrates by thermal evaporation method from their fabricated alloys.

2. Experimental procedure

$(\text{Cu}_{1-x}\text{Ag}_x)_2\text{ZnSnSe}_4$ alloys were prepared from their elements (Ag, Cu, Zn, Sn, and Se) with 99.999% purity obtained from Fluka company and different Ag content (0.0, 0.1, and 0.2). These components were weighted according to exacting the atomic ratios which corresponding to different alloys and then put in clean quartz tubes after mixing with each other. Under 10^{-3} Torr vacuum the tubes were sealed. The tubes were placed into electric furnace after placed them into containers. The temperature was increased in steps until reached 1373K, where the samples stayed in it for 7h. At last the tubes quickly were taken out and immersed in cold water to make rapid quenching for samples. The ingots were taken out from tubes and powdered very well to usage for preparing thin $(\text{Cu,Ag})_2\text{ZnSnSe}_4$ films on cleaned glass substrates at room temperature with thickness of 800 nm and deposition rate of 0.53nm/sec by vacuum evaporation method using Edward vacuum coating under vacuum of 10^{-5} Torr. Finally thin films were annealed in vacuum at (373, and 473)K.

The crystal structure of prepared alloys and all thin films was distinguished by using XRD method using radiation from $\text{CuK}\alpha$ radiation target and using SHIMADZU XRD- 6000 diffractometer.

The interplanar spacing (d_{hkl}) of miller index (hkl) was estimated by using Bragg's law [18]:

$$2d_{hkl}\sin\theta = n\lambda \quad (1)$$

Where θ is incident angle, λ is the X-ray wave length, and n is the diffraction order.

Also from XRD, we can calculate the average crystallite size (C.S) by using Scherer's equation [19]:

$$C.S = \frac{0.9\lambda}{B\cos\theta} \quad (2)$$

Where B is the (FWHM) full width at half maximum, θ is the Bragg's angle.

Furthermore the lattice constant (a, and c) of this system can be obtained from standard equation [20]:

$$\frac{4\sin^2\theta}{\lambda^2} = \frac{h^2 + k^2}{a^2} + \frac{l^2}{c^2} \quad (3)$$

The surface topography of as deposited and annealed thin CAZTSe films was examined by using Atomic Force Microscopy (AA3000), (Scanning probe microscope (SPM)).

3. Result and discussion

Fig. 1 displays the X-ray diffraction spectra of $(\text{Cu}_{1-x}\text{Ag}_x)_2\text{ZnSnSe}_4$ alloys with $0 \leq x \leq 0.2$. From this figure we can notice that the spectrum for $x=0$ ($\text{Cu}_2\text{ZnSnSe}_4$) adopts five polycrystalline peaks equivalent to reflection from (112), (204), (312), (008), and (316) planes of tetragonal phase having a kesterite type as compared with ICDD card (00-052-0868) of CZTSe. While the spectra of CAZTSe alloys for $x=0.1$, and 0.2 exhibit only three polycrystalline peaks equivalent to reflection from (112), (204), and (316) planes, which return to CAZTSe tetragonal phase, having a

kesterite type as compared with results were obtained by Weiyan et al. [21]. These spectra confirm that CAZTSe alloys with $0 \leq x \leq 0.2$ could be successfully fabricated. Also, it is observed from figure 1 the major peak (112) becomes sharper and more intensity with increase x . Furthermore, from these spectra and Table 1 which summarized the magnitude of XRD parameters, it can be seen that the peaks shift to lower Bragg's angle with increase x , this what also emphasized by Weiyan et al. [21]. Therefore, the interplanar spacing (d_{hkl}) which determined by using equation (1), expands with increase x . Also, it is clear that when x increase the magnitude of FWHM of major peak (112) shrinks, therefore the C.S which estimated form FWHM of major peak by using relationship (2), increased with increase x . This is as a result from replacement of Cu with ionic radius (0.91 \AA) by Ag which possesses a larger ionic radius (1.29 \AA) [17], that means the increase in Ag content led to amelioration in crystal structure and reducing in crystalline defects. Also, the magnitude of lattice constants which is determined by using relationship (3) expanded with increase x . This result in agree with Lupan et al. [22].

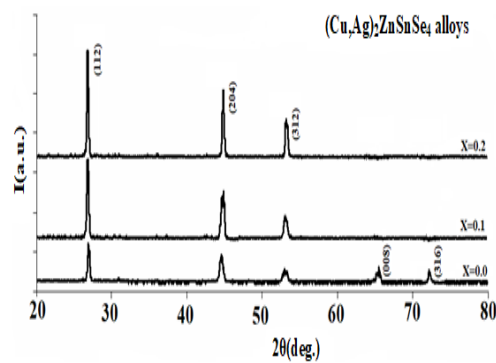


Fig. 1. XRD spectra of $(\text{Cu,Ag})_2\text{ZnSnSe}_4$ alloys.

Table 1. XRD parameters of $(\text{Cu,Ag})_2\text{ZnSnSe}_4$ alloys.

Ag content	d(exp.) (Å)	d(stand.) (Å)	2θ (exp.) (deg.)	hkl	FWHM (deg.)	C.S (nm)	a, c exp.(Å)	a, c stand(Å)
0.0	3.2781	3.2830	27.1793	112	0.34900	23.4290	a=5.69 c=11.33	a=5.693 c=11.333
	2.0086	2.0100	45.0970	204				
	1.7238	1.7140	53.0810	312				
	1.4180	1.4170	65.8069	008				
	1.3057	1.3030	72.3024	316				
0.1	3.3116	-----	26.8993	112	0.29240	27.9477	a=5.70 c=11.35	-----
	2.0235	-----	44.7470	204				
	1.7292	-----	52.9010	312				
0.2	3.3895	-----	26.2693	112	0.22530	36.2242	a=5.75 c=11.52	-----
	2.0869	-----	43.3170	204				
	1.7545	-----	52.0810	312				

The expanding in the lattice parameter can be result from either Ag ions substitution or interstitial incorporation in the lattice [23]. It can be concluded that the c/a ratio equal to 1.99 for $\text{Cu}_2\text{ZnSnSe}_4$ which confirms that the type of $\text{Cu}_2\text{ZnSnSe}_4$ crystal structure is a kesterite as previously mentioned. This result in agree with Kaya et al. [24].

Fig. 2 (a) shows the XRD spectra of as deposited CAZTSe thin films for $0 \leq x \leq 0.2$. It can be seen that the spectrum of films without Ag adopts two peaks which correspond to reflection from (112), and (204) planes of CZTSe tetragonal phase with preferential orientation in [112] direction. This result matched with [25-27]. Also, it can be noticed that the crystal structure and orientation of as deposited thin films remain the same after adding Ag with 0.1 and 0.2 ratios, but there is shifting in major peak to lower to 2θ as compared with CZTSe thin film, and this shifting increasing with increase Ag content. This result agree with reports [17, 26, 28], and that confirms Ag occupation for Cu site in the CZTSe lattice[26]. As a result, the magnitude of d_{hkl} increases with increasing Ag ratio. Also, the increase in Ag ratio causes the decreases in FWHM of major peak which finally leads to increase in C.S of these films. The same result was obtained by Henry et al. [26].

A point of interest is that the predominate [112] direction indicate that the growth of crystallite grains occur in this direction which is parallel to substrate plane [10]. From figure 2(b, and c) which shows the XRD spectra of heat treatment thin films at 373, and 473K respectively under vacuum, it can be recognized that the behavior of annealed films is similar to that in as deposited films. But the difference between the spectra of before and after annealing is that the crystal structure alters from low crystallization to high crystallization. The crystallization improvement with increasing the annealing temperature due to the increase in C.S of these films with increasing the temperature of heat treatment, this result may be caused from nucleation formation [29]. This result agrees with Cooper et al. [30] for thin CZTSe films. It is necessary to notice that there was no additional peak returns to other compounds or elements and secondary phase, can be observed in all spectra of CAZTSe alloys and thin films.

Table (2) summarized the calculated structural parameters of as deposited and heat treatment thin CAZTSe films.

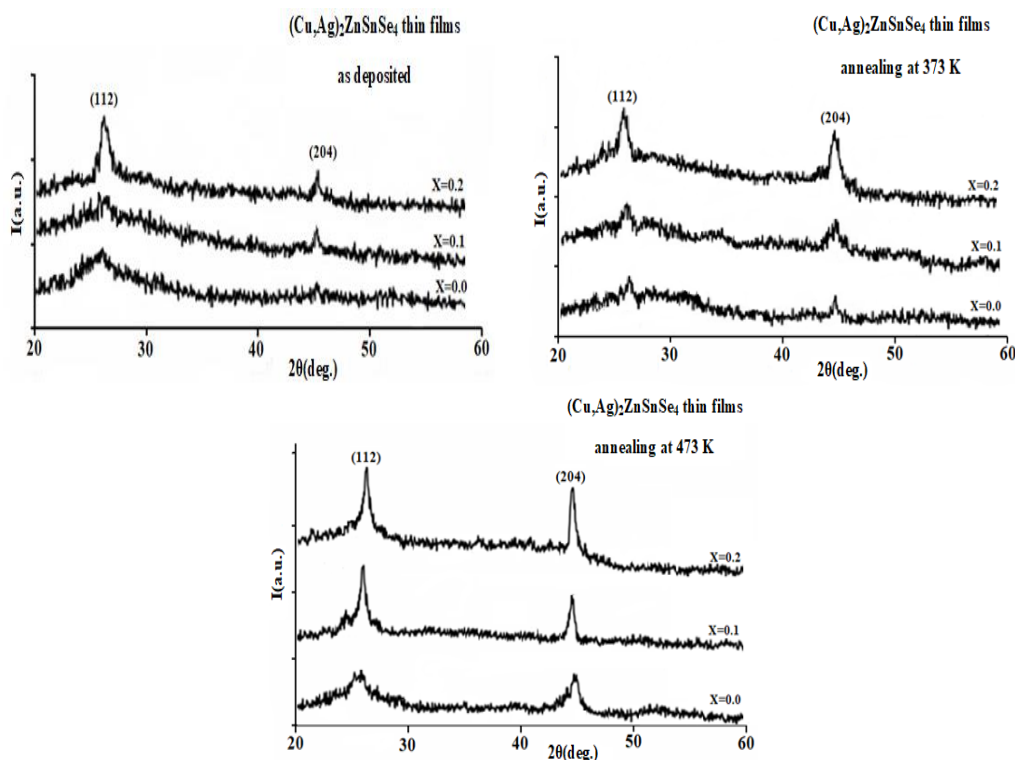


Fig. 2. XRD spectra of as deposited and annealed thin $(\text{Cu,Ag})_2\text{ZnSnSe}_4$ films at different Ag content: (a) $x=0$, (b) $x=0.1$, and (c) $x=0.2$.

Table 2. XRD parameters of thin $(Cu,Ag)_2ZnSnSe_4$ films.

x(Ag content)	Ta (K)	d(exp.) (Å)	2θ(exp.) (deg.)	hkl	FWHM (deg.)	C.S (nm)
0.0	R.T	3.3261	26.7793	112	0.669	12.2120
		2.0031	45.2270	204		
	373	3.3310	26.7392	112	0.537	15.2126
		2.0036	45.2150	204		
	473	3.3336	26.7183	112	0.470	17.3805
		2.0042	45.2011	204		
0.1	R.T	3.3507	26.5793	112	0.329	24.8221
		2.0188	44.8570	204		
	373	3.3558	26.5382	112	0.318	25.6786
		2.0212	44.8010	204		
	473	3.3584	26.5172	112	0.299	27.3092
		2.0220	44.7810	204		
0.2	R.T	3.3946	26.2293	112	0.258	31.6304
		2.0330	44.5270	204		
	373	3.3962	26.2172	112	0.208	39.2329
		2.03351	44.5160	204		
	473	3.3982	26.2011	112	0.169	48.2850
		2.0340	44.5032	204		

The effect of Ag content and annealing temperature on thin CAZTSe films surface were morphologically distinguished by using AFM technique.

Figs. 3, 4, and 5 display the 2D and 3D AFM images of all thin CAZTSe films before and after heat treatment, which confirm that all films adopt dense and homogeneous surfaces with spherical like shape particles. This result confirms the fact which estimated from XRD examine, which confirms that all films before and after heat treatment have crystalline nature. From table 3 it can be noticed that the values of grain size, surface roughness, and root mean square increase with increasing Ag content and annealing temperature. The increase in grain size agree with increase in C.S which was estimated from XRD analysis and indicates that Ag work as a flux which helps in growth of grains [31]. Large grain size causes the decrease of grain boundaries so, the centers of trapping electrons will decrease, and therefore the large grain size is very beneficial for solar cell application [29, 32].

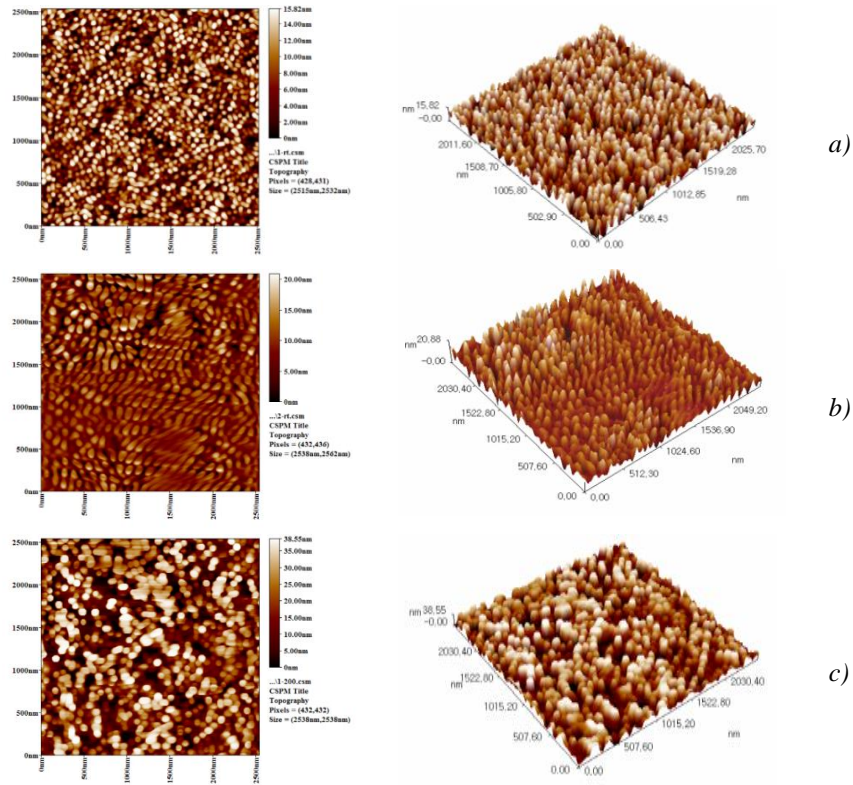


Fig. 3. The 2D and 3D AFM images of as deposited and annealed thin $Cu_2ZnSnSe_4$ films at: a) R.T, (b) 373K, and (c) 473K.

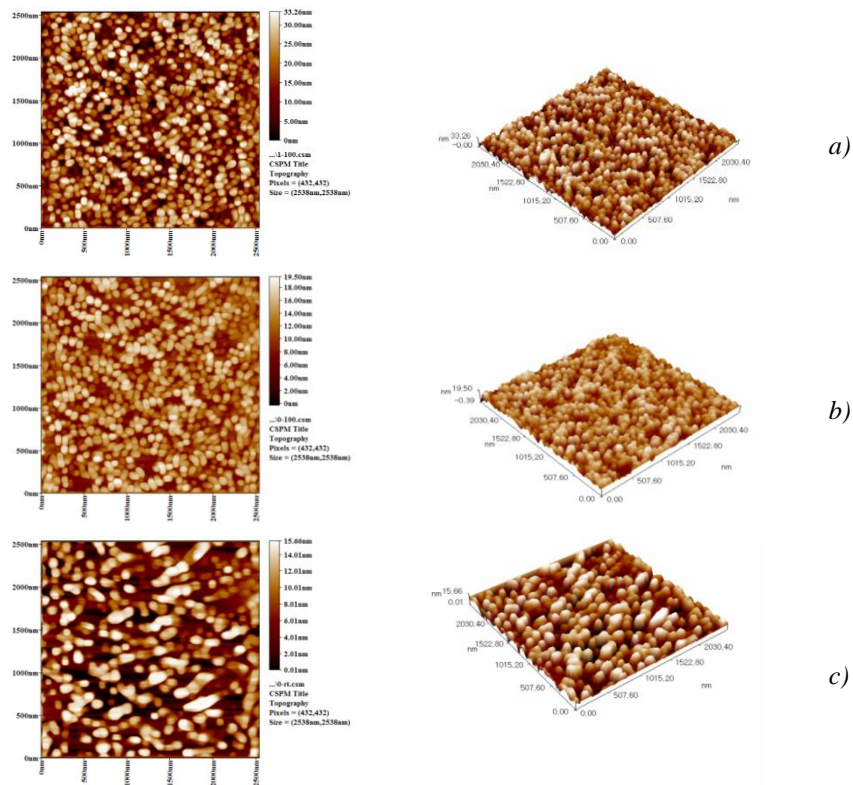


Fig. 4. The 2D and 3D AFM images of as deposited and annealed thin $Cu_{0.9}Ag_{0.1}ZnSnSe_4$ films at: a) R.T, (b) 373K, and (c) 473K.

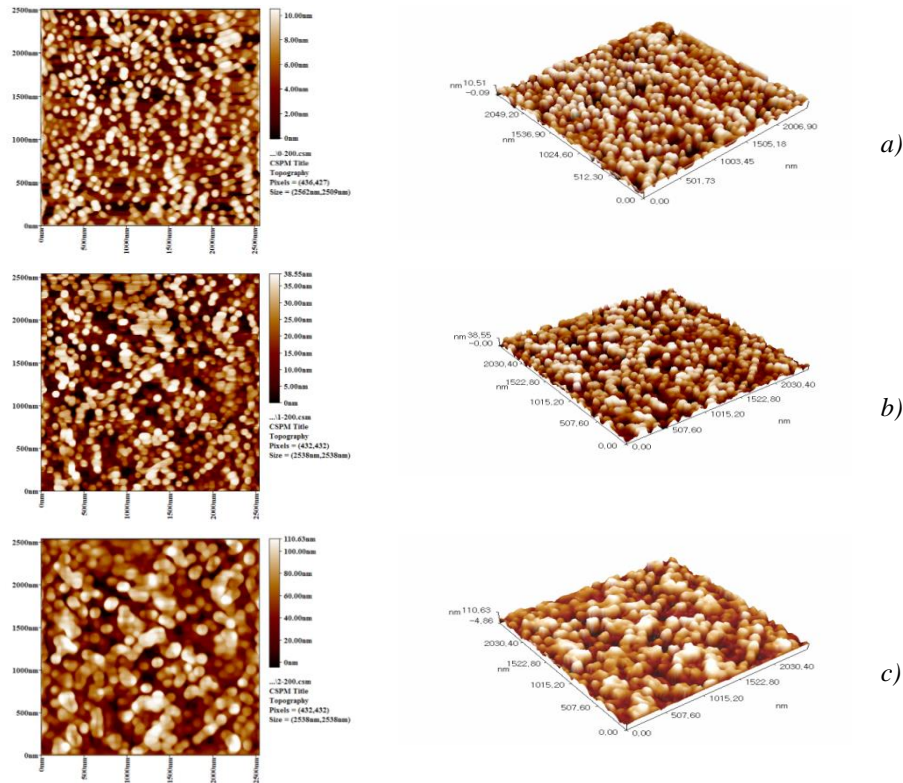


Fig. 5. The 2D and 3D AFM images of as deposited and annealed thin $\text{Cu}_{0.8}\text{Ag}_{0.2}\text{ZnSnSe}_4$ films at: (a) R.T, (b) 373K, and (c) 473K.

Table 2. The effect of Ag content and annealing temperature on AFM parameters.

x	Ta (K)	Surfaces roughness (nm)	Root mean Sq. (nm)	Grain Size (nm)
0	R.T	2.54	2.54	67.66
	373	2.72	3.23	71.75
	473	2.9	3.65	75.03
0.2	R.T	3.91	4.52	75.39
	373	3.94	4.54	77.96
	473	6.79	8.08	80.92
0.3	R.T	9.64	11.1	90.47
	373	9.66	11.3	90.52
	473	23.4	28.0	95.36

4. Conclusions

Thin CAZTSe films have been grown onto glass substrate at R.T from their prepared alloys for $0 \leq x \leq 0.2$ successfully by using thermal evaporation method. XRD analysis confirms that pure Cu thin films are polycrystalline in nature which had tetragonal phase with preferential orientation in [112] direction. Incorporation Ag in CZTSe films and annealed them under vacuum at (373, and 473) K for one hour doesn't cause any change in their crystal structure but achieve enhancement in it. Grain size, r.m.s, and surface roughness of CAZTSe films were increased with increasing of Ag content and annealing temperature as noticed from AFM measurements. So, incorporation Ag in CZTSe films is a promising way to enhance their properties to get suitable absorber layer for solar cell application.

References

- [1] J. Henry, K. Mohanraj, G. Sivakumar, *J. Phys. Chem. C* **123**, 2094 (2019).
- [2] S. S. Malia, B. M. Patil, C. A. Betty, P. N. Bhosale, Y. W. Oh, S. R. Jadkar, R. S. Devan, Y. R. Ma, P. S. Patil, *Electrochimica Acta* **66**, 216 (2012).
- [3] J. J. Scragg, J. D. Philip, L. M. Peter, G. Zoppi, I. Forbes, *Phys. Stat. Sol. B* **245**(9), 1772 (2008).
- [4] T. Tanaka, T. Nagatomo, D. Kawasaki, M. Nishio, Q. Guo, A. Wakahara, A. Yoshida, H. Ogawa, *J. of Physics and Chemistry of Solids* **66**, 1978 (2005).
- [5] J. J. Wang, J. S. Hu, Y. G. Guo, L. J. Wan, *NPG Asia Materials* **4**, e2(2012).
- [6] G. S. Babu, Y. B. K. Kumar, P. U. Bhaskar, V. S. Raja, *J. Phys. D: Appl. Phys.* **41**, 205305 (2008).
- [7] G. Suresh Babu, Y. B. Kishore Kumar, P. Uday Bhaskar, Sundara Raja Vanjari, *Solar Energy Materials & Solar Cells* **94**, 221 (2010).
- [8] M. Gancheva, L. Kaupmeesa, J. Iliyana, J. Raudojaa, O. Volobujevaa, H. Dikovb, M. Altosaara, E. Mellikova, T. Varemaja, *Energy Procedia* **2**, 65 (2010).
- [9] O. Volobujeva, S. Bereznev, J. Raudoja, K. Otto, M. Pilvet, E. Mellikov, *Thin Solid Films* **535**, 48 (2013).
- [10] Rachmat Adhi Wibowo, Eun Soo Lee, Badrul Munir, Kyoo Ho Kim, *Phys. Stat. Sol. A* **204**(10), 3373 (2007).
- [11] G. M. Ilari, C. M. Fella, C. Ziegler, A. R. Uhl, Y. E. Romanyuk, A. N. Tiwari, *Sol. Energy Mater. Sol. Cells* **104**, 125 (2012).
- [12] A. W. Rachmat, S. K. Woo, S. L. Eun, M. Badrul, H. K. Kyoo, *Journal of Physics and Chemistry of Solid* **68**, 1908 (2007).
- [13] Fang-I Lai, Jui-Fu Yang, Yu-Ling Wei, Shou-Yi Kuo, *Green Chem.* **19**, 795 (2017).
- [14] Shiyong Chen, X. G. Gong, Aron Walsh, Su-Huai Wei, *Applied Physics Letters* **94**(041903), 1 (2009).
- [15] T. Gershon, K. Sardashti, Y. S. Lee, O. Gunawan, S. Singh, D. Bishop, A. C. Kummel, R. Haight, *Acta Mater.* **126**, 383 (2017).
- [16] A. Guchhait, Z. Su, Y. F. Tay, S. Shukla, W. Li, S. W. Leow, J. M. R. Tan, S. Lie, O. Gunawan, L. H. Wong, *ACS Energy Letters* **1**, 1256 (2016).
- [17] T. Gershon, Y. S. Lee, P. Antunez, R. Mankad, S. Singh, D. Bishop, O. Gunawan, M. Hopstaken, R. Haight, *Adv. Energy Mater.* **6**(10), 1502468 (2016).
- [18] B. D. Cullity, *Elements of X-ray diffraction*, Addison-Wesley Pub. Co. Ind., London, 1967.
- [19] B. U. Maheshwari, V. S. Kumar, *Int. J. Energy Res.* **39**, 771 (2015).
- [20] H. P. Klug, L. E. Alexander, *X-ray diffraction procedure*, John Wiley & Sons, New York, USA, 1974.
- [21] W. Gong, T. Tabata, K. Takei, M. Morihama, T. Maeda, T. Wada, *Phys. Status Solidi C* **12**(6), 700 (2015).
- [22] O. Lupan, L. Chow, L. O. Ono, B. R. Cuenya, G. Chai, H. Khallaf, S. Park, A. Schulte, *J. Phys. Chem. C* **114**, 12401 (2010).
- [23] A. N. Gruzintsev, V. T. Volkov, E. E. Yakimov, *Semiconductors* **37**(3), 259 (2003).
- [24] K. Wei, A. R. Khabibullin, T. Stedman, L. M. Woods, G. S. Nolas, *J. of Applied Physics* **122**, 105109 (2017).
- [25] T. Tanaka, T. Sueishi, K. Saito, Q. Guo, M. Nishio, K. M. Yu, W. Walukiewicz, *Journal of Applied Physics* **111**(053522), 1 (2012).
- [26] J. Henry, K. Mohanraj, G. Sivakumar, *J. Vacuum* **160**, 347 (2019).
- [27] L. Yao, J. Ao, M. J. Jeng, J. Bi, S. Gao, G. Sun, Q. He, Z. Zhou, Y. Zhang, Y. Sun, L. B. Chang, *Crystals* **9**(10), 1 (2019).
- [28] H. O. Bian, S. Y. Ma, F. M. Li, H. B. Zhu, *Superlattices and Microstructures* **58**, 171 (2013).
- [29] J. Henry, K. Mohanraj, G. Sivakumar, *Vacuum* **156**, 172 (2018).
- [30] C. S. Cooper, P. Arnou, L. D. Wright, S. Ulicna, J. M. Walls, A. V. Malkov, J. W. Bowers, *Thin Solid Films* **633**, 151 (2017).
- [31] M. S. Kumar, S. P. Madhusudanan, S. K. Batabyal, *Solar Energy Materials and Solar Cells* **185**, 287 (2018).

- [32] H. Guo, Ch. Ma, K. Zhang, X. Jia, Y. Li, N. Yuan, J. Ding, *Solar Energy Materials and Solar Cells* **178**, 146 (2018).